tion of the volume during pressure relief is preferable to that during pumping, since during pumping there is possible a leakage of the working fluid through the sealing of the stock of the pump.

For measuring pressure, a manganin sensor is used or, to be more precise, four pieces of a wire connected into a bridge circuit located in the same housing in the 'cold' zone, outside the heater. Two elements of the bridge (located along the diagonal) are placed in the high pressure; zone two others, in the normal pressure zone. This variant of the connection makes it possible to increase the sensitivity by a factor of two in comparison with a single manganin sensor in the high pressure zone and to considerably decrease the temperature dependence, since all the elements of the bridge are located at one and the same temperature.

The presence of a pump and a membrane separator makes it possible to prepare a mixture of a given concentration in the measuring cell. In the filling process, the pressure in the cell grows to the maximum value (at room temperature). Preliminarily, the pressure dependence of the volume of the displaced liquid during pressure relief with an unfilled measuring cell $L_0(P)$ is recorded for the selected working fluid. The registration of the same dependence with a filled measuring cell $L_1(P)$ makes it possible to determine the volume occupied by the substance under investigation, depending on pressure, i.e., to find the function $\rho(T_0, P)$. For determining the equation of state of a mixture $\rho(T, P)$, the data on the isothermal compressibility at room temperature are supplemented by the results of measurements of the temperature dependence of pressure during the warming-up of the measuring cell under isochoric conditions at different initial pressures.

In the measuring cell, there are sensors for measuring viscosity, thermal conductivity, and electrical conductivity. For measuring viscosity, the vibration viscosimeter method, i.e., the registration of frequency and damping of free vibrations of a rod after impact excitation, is used. The impact excitation is performed by applying a rectangular current pulse to one of two electromagnets. The recorded signal is proportional to the angle of deflection of the rod. For thermal-conductivity measurements, the method of a heated wire is used. The electrical conductivity is determined based on the current between two plates to which a voltage is applied.

References

1. Joule J P *Philos. Mag.* **17** 364 (1859)
2. Boehler R, Getting C, Kennedy G C *J. Phys. Chem. Solids* **38** 233 (1977)
3. Dzhavadov L N, Krotov Yu I *Fiz. Tverd. Tela* **22** 1245 (1980) [*Sov. Phys. Solid State* **22** 728 (1980)]
4. Boehler R, Ramakrishnan H *Geophys. Res.* **85** (B12) 6996 (1980)
5. Dzhavadov L N, Krotov Yu I *Prib. Tekh. Eksp.* (3) 168 (1985)
6. Dzhavadov L N *Fiz. Tverd. Tela* **27** 3310 (1985) [*Sov. Phys. Solid State* **27** 1993 (1985)]
7. Dzhavadov L N *Zh. Fiz. Khim.* **61** 1106 (1987)
8. Dzhavadov L N *High Temp. High Press.* **21** 401 (1989)
9. Dzhavadov L N *Fiz. Tverd. Tela* **47** 2223 (2005) [*Phys. Solid State* **47** 2315 (2005)]
10. Voronov F F, Grigor'ev S B *Byull. Izobret. SSSR* (2) 142 (1972)
11. Khvostantsev L G, Vereshchagin L F, Novikov A R *High Temp. High Phys.* **9** 637 (1977)
12. Voronov F F, Goncharova V A, Stal'gorova O V *Zh. Eksp. Teor. Fiz.* **76** 1351 (1979) [*Sov. Phys. JETP* **49** 687 (1979)]
13. Voronov F F *Adv. Space Res.* **1** 147 (1981)
14. Goncharova V A, Chernysheva E V, Voronov F F *Fiz. Tverd. Tela* **25** 3680 (1983) [*Sov. Phys. Solid State* **25** 2118 (1983)]
15. Goncharova V F, Chernysheva E V *Semicond. Sci. Technol.* **4** 114 (1989)
16. Voronov F F, Stal'gorova O V, Gromnitskaya E L *Zh. Eksp. Teor. Fiz.* **122** 90 (2002) [*JETP* **95** 77 (2002)]
17. Gromnitskaya E L, Stal'gorova O V *Zh. Eksp. Teor. Fiz.* **106** 1453 (1994) [*JETP* **79** 785 (1994)]
18. Stal'gorova O V et al. *Prib. Tekh. Eksp.* **39** (6) 115 (1996) [*Instrum. Exp. Tech.* **39** 880 (1996)]
19. Gromnitskaya E L et al. *Phys. Rev. B* **64** 094205 (2001)
20. Lyapin A G et al. *Zh. Eksp. Teor. Fiz.* **121** 335 (2002) [*JETP* **94** 283 (2002)]
21. Gromnitskaya E L et al. *Phys. Rev. Lett.* **98** 165503 (2007)
22. Wijngaarden R J *High Press. Res.* **3** 105 (1990)
23. Mao H K et al *J. Appl. Phys.* **49** 3276 (1978)
24. Kankeleit E *Rev. Sci. Instrum.* **35** 194 (1964)

PACS numbers: **01.65.+g**, **71.18.+y**, **73.20.–r**
DOI: 10.1070/PU2008v051n10ABEH006618

Quantum transport at high pressures

E M Dizhur, V A Venttsel, A N Voronovskii

Unlike other areas of condensed state physics — which can be classified according to the objects of their study (for example, the physics of semiconductors) or according to the nature of the phenomena studied (magnetism) — what unifies high pressure physics is the common investigation method, the use of high pressure to study the physical properties of various objects.

Measurements of the pressure dependence of electron transport as a means to probe physical models of condensed state were started at the Laboratory of Electric and Galvanomagnetic Phenomena headed by A I Likhter, which has been part of the Institute for High Pressure Physics, RAS (IHPP) since the very foundation of the institute in 1958.

Coincident with the foundation of the institute was a spurt in the study of electron energy spectra in metals. It was during that time that the school of I M Lifshitz came to prominence with its advances in solid state theory and it was then that Fermi surfaces (FSs) of normal metals started to be extensively studied. The application of high pressure to these studies was pioneered by IHPP scientists as early as 1963, in a work [1] that provided experimental data on the resistivity, the Hall constant, and the magnetoresistivity of graphite under a pressure of up to 1 GPa at temperatures from room temperature to 450 K. By comparing the experimental data with the analytical expressions for the galvanomagnetic properties of graphite, it proved possible to separate lattice-related effects (relaxation time) from those related to conduction electrons and to refine the energy spectrum parameters underlying the theoretical model used.

In the next major development, E S Itskevich and his Oscillation Phenomena Group (later to become the Laboratory of Quasiparticle Energy Spectra) succeeded in observing a change in the behavior of magnetoresistance in cadmium that confirmed the earlier prediction of a change in the FS topology [2]. Later, in Ref. [3], a direct measurement of the de Haas – van Alphen effect under a pressure of up to 2 GPa revealed the emergence of a new FS cross section in cadmium [3].

Zinc and cadmium have very similar electronic properties. In fact, from this viewpoint they are only different in the value

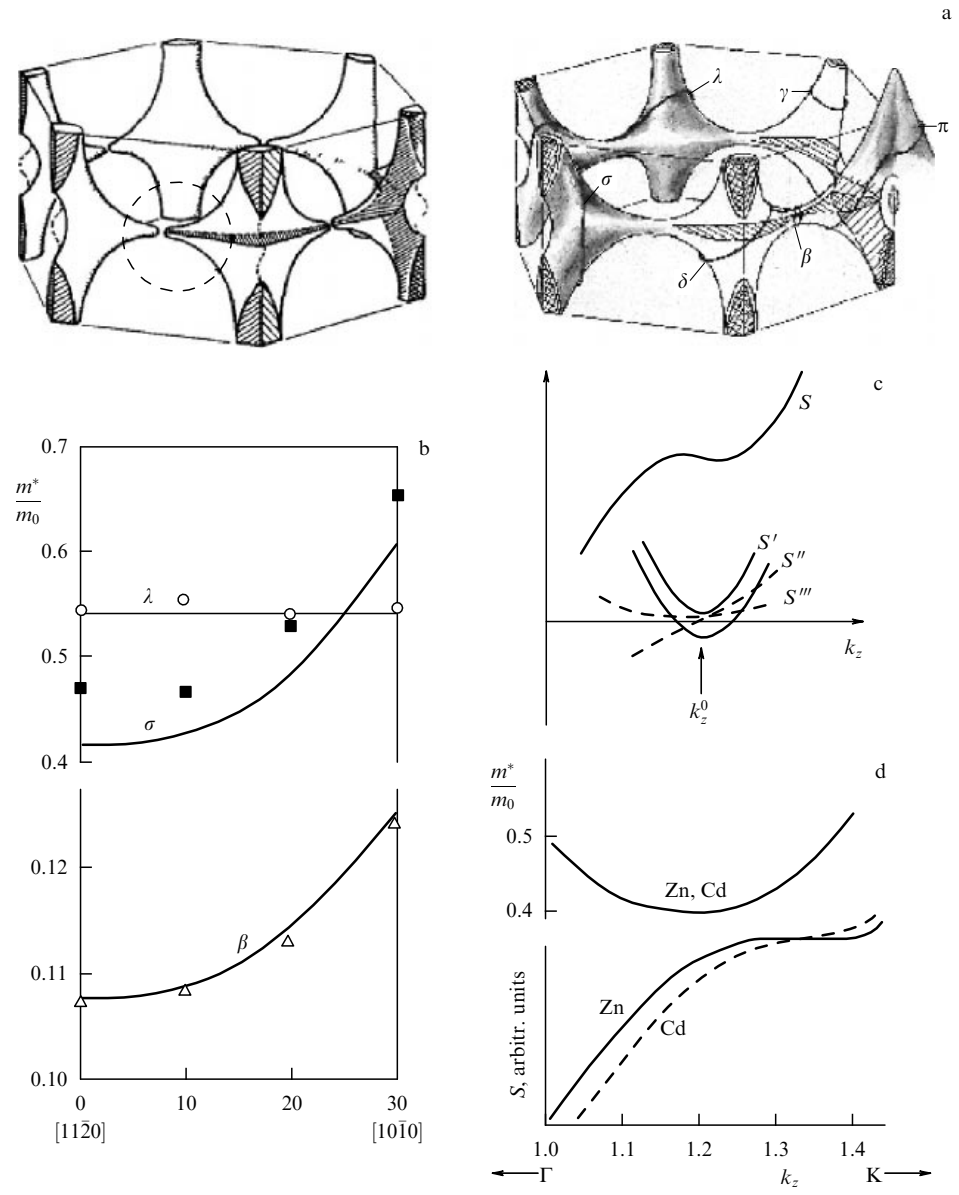

Figure 1. (a) Fermi surface of cadmium (left) and zinc (right) at normal pressure. When under pressure, the cadmium FS acquires a neck (in the circled region). (b) Comparison of de Haas – van Alphen (symbols) versus cyclotron resonance (solid lines) effective masses for various portions of FS. (c) Special section $S(k_z)$ and its derivatives. (d) Special sections and their effective masses.

of the axis ratio c/a. As cadmium is compressed, its c/a ratio approaches that of zinc, for which reason it was quite appropriate to study the properties of both. The nearly free electron models of zinc and cadmium Fermi surfaces are very realistic. Magnetic breakdown experienced by narrow energy gaps in the spectra of these metals lead to a very complex picture of FS cross sections as a function of the orientation and magnitude of an applied magnetic field. Band structure calculations show that using the nonlocal approximation and taking into account the influence of the d band results in the disappearance in the third and fourth zones of very large electron portions of the Fermi surface near the L-point of the Brillouin zone. To obtain a correct band structure, systematic studies were performed at normal and high pressures. The fundamental question of whether electron portions of the FS do or do not exist near the L-point was resolved in the negative (thus strengthening the nonlocal model) by simply analyzing the sign and magnitude of the baric coefficients of the FS that could be identified with the oscillation frequencies observed.

Direct information about the FS shape and how it deforms with pressure can be obtained from oscillation phenomena. The development of techniques for de Haas – van Alphen effect measurements in pulsed and stationary magnetic fields under hydrostatic pressure [4] has made it possible to measure, under true hydrostatic conditions, the shift in the oscillation phase, a quantity directly related to the baric coefficient of the FS cross section area $\mathrm{d}\ln S/\mathrm{d}P$. Precision measurements showed that the effective mass m^* corresponding to the new pressure-produced FS cross section in Cd differs markedly from the cyclotron resonance value of m^* [5]. It was assumed that this new cross section was analogous to the σ section of the zinc 'monster' (Fig. 1). A detailed analysis performed for zinc showed that the effective

mass for any other cross section does not depend on the measurement method used, whereas that for σ does.

Analysis of all the related phenomena led to the conclusion that the cross section σ of the monster is a *special section* of the Fermi surface. A theory of the de Haas – van Alphen effect developed for special cross sections [6] showed that for such a section the first derivative of the section area S at quasimomentum $p_z = p_z^0$ is nonzero (the section is not extremal), but the second derivative vanishes. For this special section, major changes occur in the Lifshitz – Kosevich expression for the oscillating magnetic moment — in particular in the form of an oscillating Airy function term,

$$\mathrm{Ai}\left[\left(\frac{nc}{e\hbar H}\right)^{2/3}\left(\frac{2}{S'''}\right)^{1/3}S'\right],$$

where n is the electron density, e is the electron charge, $\hbar$ is the Planck constant, c is the speed of light, H is the magnetic field, and S' (S''') is the first (third) derivative of the section area. If the argument is positive, the Airy function falls off exponentially, and if the argument is negative it oscillates, i.e., its behavior is determined by the sign of the product $S'''S'$. In zinc this sign is negative, and the σ section is well observed and demonstrates a nonmonotonic magnetic field dependence of the oscillation amplitude. In cadmium, where under normal conditions $S'''S' > 0$, the applied pressure deforms the monster and makes $S'''S'$ negative. Calculations show that the effective mass is extremal at quasimomenta other than those producing the special section. The reason for this is that, whereas the de Haas – van Alphen mass is associated with the special section, that observed in the cyclotron resonance is the extremal effective mass. That is why the two masses are markedly different (see Fig. 1).

A transition due to a change in the FS topology can be called an electron phase transition of order 2.5, and the appearance at this transition of a new branch in the electron density of states results in all kinetic phenomena starting to show some special features in their behavior. In investigating these phenomena, one of the most sensitive and relatively simple methods has proved to be thermal-EMF measurements under pressure, an approach in which various types of transitions can be distinguished. By measuring the temperature dependences of the longitudinal and transverse thermal EMF of cadmium in the 4 to 300 K temperature range under a pressure of up to 3 GPa [7], it was found that for $P < 1.2$ GPa

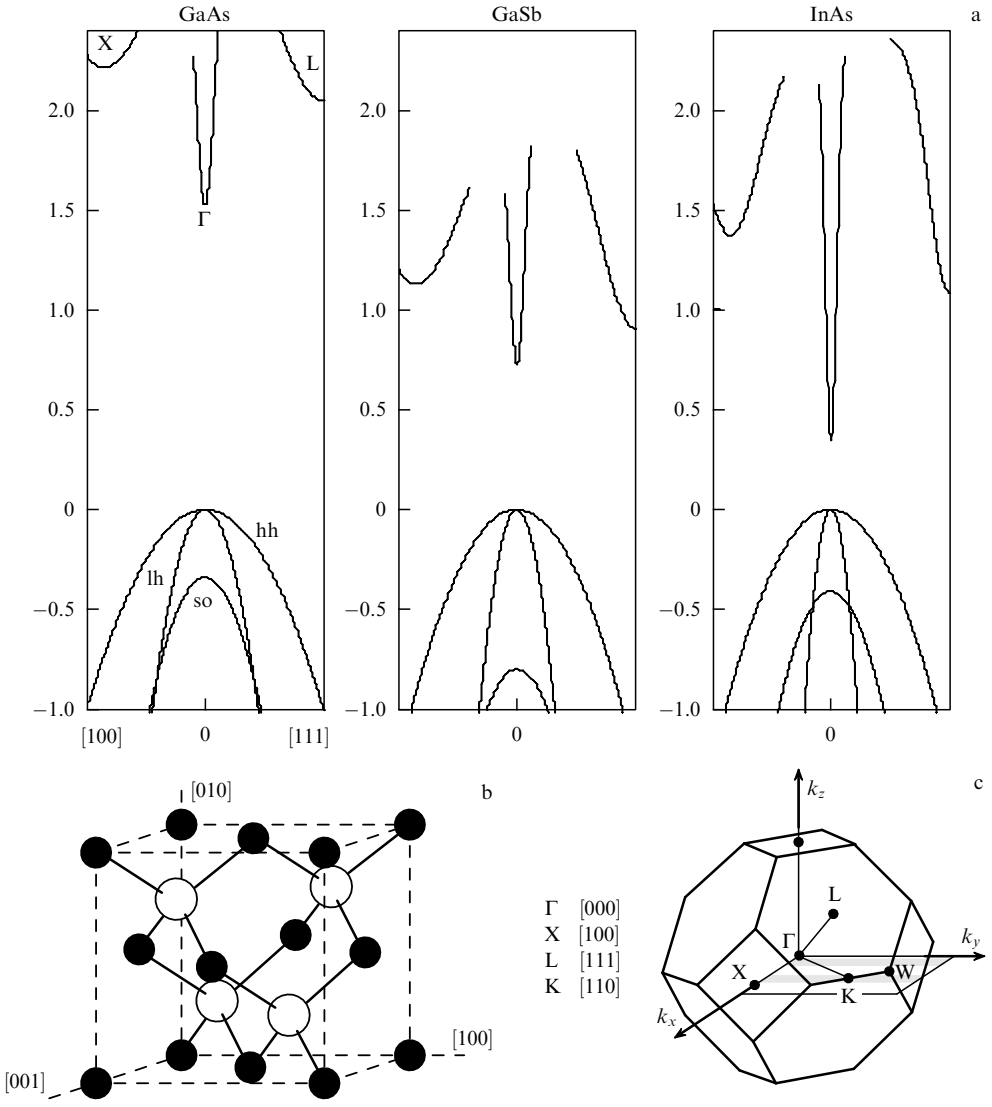

Figure 2. (a) Pressure effect on the band structure of some $A^{\mathrm{III}}B^{\mathrm{V}}$ compounds; lh (hh) is the light (heavy) hole band, so is the spin-orbit split band. (b) GaAs unit cell: ●, Ga; ○, As. (c) High-symmetry points in the first Brillouin zone.

the two curves are more or less similar, but for $P > 2$ GPa the transverse thermal EMF curve shows a positive sign anomaly. An important observation was a positive spike in the thermal EMF due to the order 2.5 transition — i.e., due to the appearance of a hole neck.

Studies of order 2.5 phase transitions have not only proved their existence but also have greatly expanded the arsenal of measurement tools suitable for high pressure conditions — expanding, in turn, the scope of studies and promoting high pressures as an instrumental means to address problems of topical interest in solid state physics. These methodological developments, along with the resistive, galvanomagnetic, and thermoelectric measurements already mentioned, include tunneling, electron-optical, and neutron diffraction measurements.

Low-temperature high-pressure studies of Pb/Al, Sn/Al, and In/Al tunnel junctions have identified those of then existed models that were the best for describing the relation between the critical temperature and the directly measured superconducting gap [8].

Methodologically, one distinguishes two subranges in the pressure range used in low-temperature electron transport studies: up to 3 GPa (hydrostatic pressure) and from 3 GPa to megabar pressures ('quasihydrostatics'). Accordingly, our studies use two types of high-pressure cells: a fixed-pressure cylinder – piston cell and a toroid cell which is loaded (at room temperature) using a minipress placed directly in the cryostat. While in cells of the first type advanced measurement techniques can be adapted relatively simply to high pressure conditions, in the range up to 3 GPa the scope of study is limited by the need to work with pressure-sensitive objects — primarily, semiconductor and semimetal systems, where pressure-induced changes in the energy bands are on the scale of the carriers' Fermi energy.

Characteristic from this point of view is the behavior of tetrahedrically bonded semiconductors, i.e., Ge and Si, as well as $A^{III}B^{V}$, almost all $A^{II}B^{VI}$, and some $A^{I}B^{VII}$ compounds. All these semiconductors have a multivalley conduction band consisting of a spheroid centered at the Γ-point of the Brillouin zone, six ellipsoids centered at the X-points, and eight semi-ellipsoids at the L-points. While for all these FS sheets the pressure-induced energy shifts of the corresponding valleys are almost the same, with respective pressure coefficients of 10, −1, and 5 meV kbar^{-1}, at normal pressure the relative energy positions of the sheets vary (Fig. 2). For example, in GaAs the energy gap is direct (a minimum at Γ), whereas Ge and Si are, respectively, L-valley and X-valley semiconductors with an indirect gap, implying that a pressure of 2 GPa can, for example, transform the band structure of Ge into that of Si. (This fact was used in high-pressure tunneling measurements on Ge to determine the macroscopic Grüneisen constants for the [111] and [100] phonon branches [9].)

New and broad prospects were opened up by the application of high pressures to the study of a two-dimensional electron gas in GaSb/InAs/GaSb quantum wells. In such a well, in the absence of pressure, the conduction band edge of InAs is below the valence band edge of GaSb, so that the system develops spatially separated electron-hole layers within itself, the ionization of surface states on the interface resulting in the electron concentration in the well exceeding the hole concentration in the barriers. When pressure is applied, the bottom of the well goes up, leading to the disappearance of holes, after which, as the bottom of the well approaches the surface state level, the electron concentration falls to zero (Fig. 3). Such a pressure-induced transition from a 'semimetal' two-carrier-type state to a 'semiconductor' one-carrier-type state, and further to the insulating state, has been observed in magnetoresistance

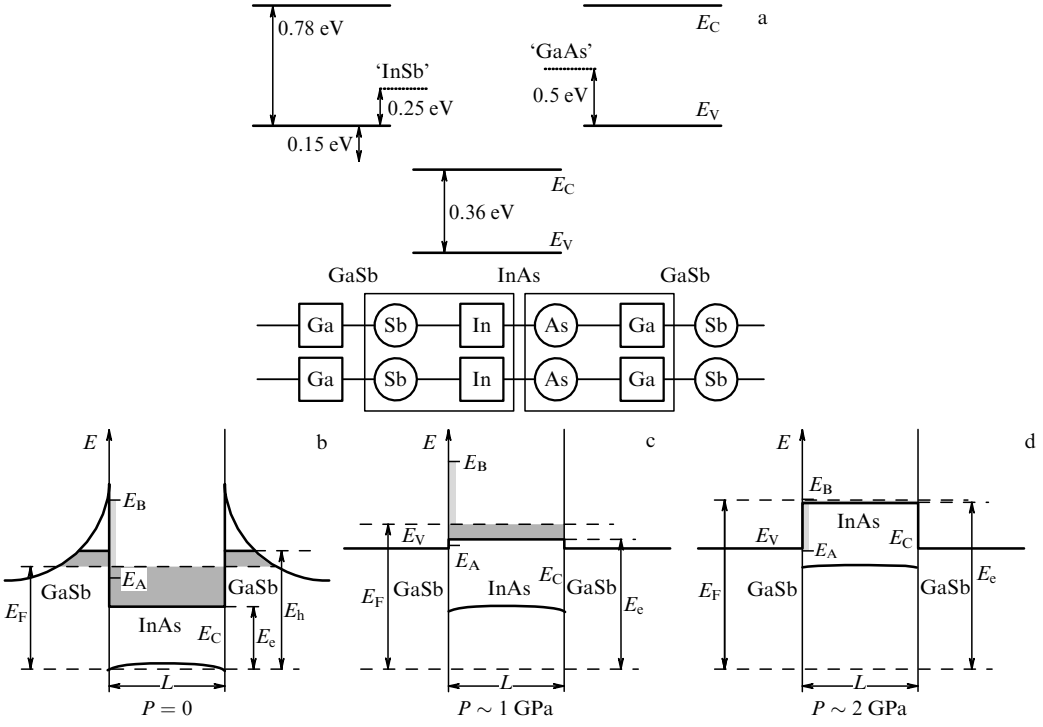

Figure 3. (a) Band edge diagram for a GaSb/InAs/GaSb quantum well and the formation of two types of interfaces. (b – d) Schematics for the effect of pressure and surface donor states on carrier concentration. E_V' (E_C) is the valence (conduction) band; E_B (E_A) is the band of bonding (antibonding) states; E_e (E_h) is the first band of quantum confinement of electrons (holes); E_F is the Fermi level.

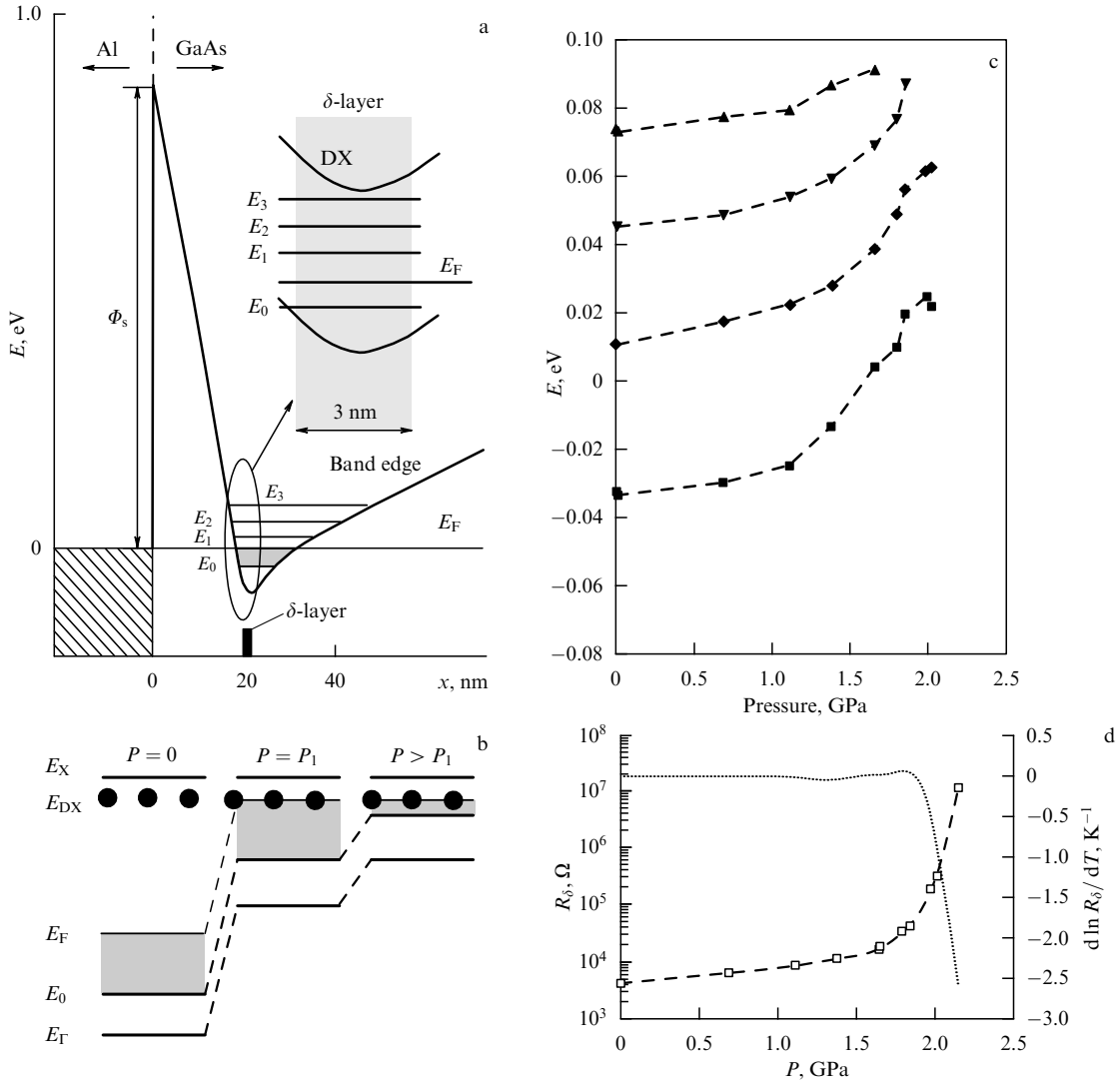

Figure 4. (a) Interface potential profile and the system of quantum confinement levels. (b) Pressure-induced change in the relative position of major energy levels; E_X, the edge of the X valley; E_{DX}, the level of DX centers; E_F, Fermi level; at a pressure P_1 the Fermi level becomes coincident with that of the DX centers, E_0 is the edge of the lower quantum confinement subband, $E_{1,2,3}$ are the successive quantum confinement bands, Φ_s is the potential barrier height, E_Γ is the conduction band edge (Γ valley). (c) Pressure dependence of the positions of quantum confinement subbands as obtained from tunneling spectra. (d) Pressure dependences of resistance R_δ (−□−) and the temperature resistance coefficient of the δ layer (dotted line).

oscillations under pressure. Furthermore, because varying the layer deposition sequence in the molecular-beam epitaxy allowed two types of interface — 'GaAs' and 'InSb' — to be formed, the spectra of surface states for both interface types were determined from high pressure measurements [10].

The above approach of varying carrier concentration by applying high pressure at a constant level of doping was used further in the study of the two-dimensional electron system in near-surface Si δ doped GaAs [11]. In this study, advantage was taken of the fact that substitutional impurities (Si, Sn, and Te) form so-called DX centers, whose position is tied to the conduction band X valley. Due to the Γ valley approaching the DX center level, quantum well electrons localize on the latter and so reduce in concentration, thus enhancing the role of interaction and reducing correlation (Fig. 4). By simultaneously measuring the resistance of the δ layer and the spectra of normal tunneling to the δ layer it was shown that this metallic-to-diffusion conduction crossover produces a density-of-states gap at the Fermi level. It should be noted that, unlike magnetotransport measurements, tunneling not only pinpoints the position of the filled levels of quantum confinement but also determines the way in which the unfilled upper-lying quantum confinement levels change their position with pressure.

A further possible application of high-pressure techniques is to vary the effective dimensionality when studying the one-dimensional systems of the family MX_3 (M = Ta, Nb; X = S, Se). The substances of this group are highly anisotropic three-dimensional (3D) conductors consisting of conducting chains weakly bonded by van der Waals forces. Unlike 3D metals, whose electron properties are well described by Landau Fermi liquid theory, a one-dimensional (1D) system has no electron excitations, and those elementary excitations present are collective charge and spin modes. This state is called a Luttinger liquid. On the other hand, in quasi-one-dimensional conductors the electron – phonon interaction usually leads to a Peierls phase transition, resulting in the appearance of a charge-density-wave (CDW) state. It had been known that MX_3 compounds vary considerably in their electron properties. For example, $TaSe_3$ is a metal; $NbSe_3$, while

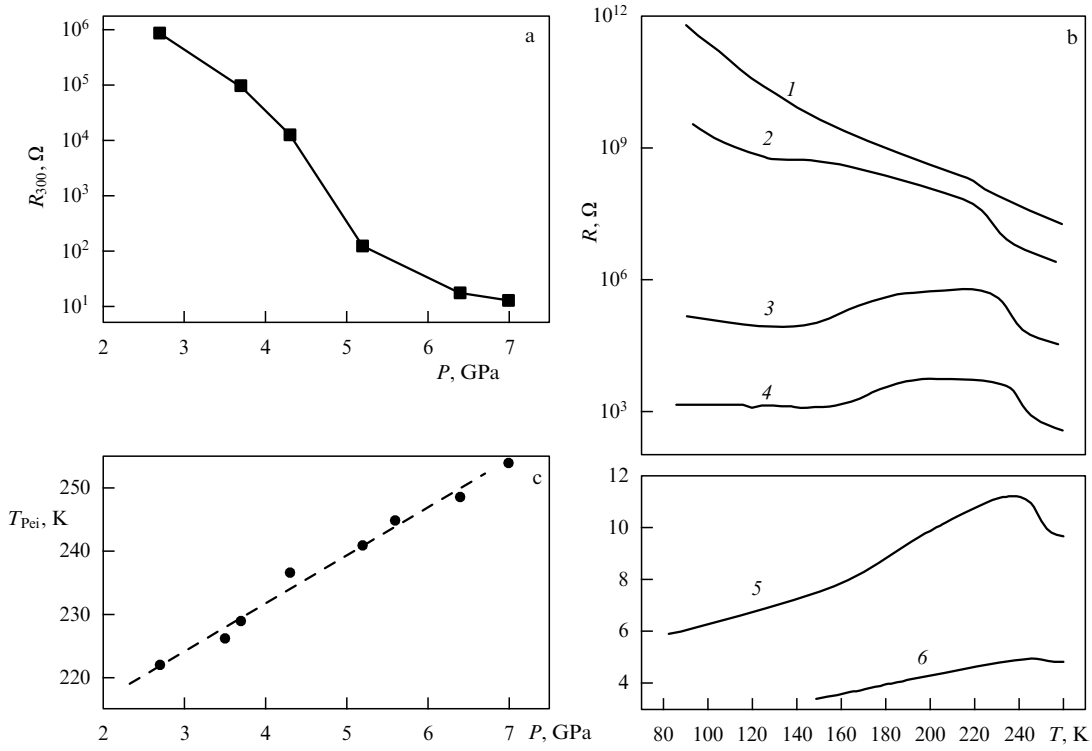

Figure 5. (a) Resistance versus pressure for NbS_3 at room temperature. (b) Resistance versus temperature for NbS_3 at pressures in GPa of 2.7 (*1*), 3.7 (*2*), 4.3 (*3*), 5.2 (*4*), 6.4 (*5*), and 7.0 (*6*). (c) Peierls transition temperature as a function of pressure. Dashed line is for $T^* \approx 7.5P + 202$.

undergoing CDW-forming transitions, remains metal-conducting at low temperatures; in TaS_3, the formation of CDW at 220 K makes the electron spectrum fully dielectricized; NbS_3 exhibits dielectric properties at both low and room temperatures. Thus, the metallic nature of conduction is enhanced in the order $NbS_3 \rightarrow TaS_3 \rightarrow NbSe_3 \rightarrow TaSe_3$.

At the Institute of Radioengineering and Electronics, RAS, the temperature and field dependences of conductivity were obtained for quasi-1D TaS_3 and $NbSe_3$ with cross sections of tens to hundreds of nm, which revealed a transition in these conductors from metallic (3D) behavior at room temperature to nonmetallic (1D) behavior below 50–100 K, with the CDW state either disappearing or surviving in the transition, and which also showed that the smaller the cross section of the thread-like crystals, the weaker the metallic nature of the conductivity. It was therefore of interest for us to see how pressure affects the conductivity of a quasi-1D 'insulator' NbS_3, with a view to reduce the chain-to-chain separation and to test the current understanding of the physical conduction mechanism. This understanding is that impurities in 1D chains form tunnel barriers that break the chains into segments and that a Luttinger-liquid state can exist if the electron hopping integral between the chains is smaller than the quantum confinement energy in the chain segments between the impurities. Because the hopping integral should increase with pressure, it was reasonable to expect that increasing pressure should cause the disappearance of CDWs and a transition to 3D behavior. Such behavior was indeed first observed in experiments on thread-like crystals of NbS_3 [12], in which applying a hydrostatic pressure of 6 GPa produces an increase in room temperature conductivity of more than five orders of magnitude and causes the temperature resistance coefficient to change sign. Another observed feature is a jump in the resistance versus temperature curve, which brings to mind the Peierls transition and whose position depends linearly on the temperature (Fig. 5).

In the quasihydrostatic pressure range, the occurrence of structural phase transitions allows the experimental study of even such objects that do not really exist under normal conditions. Work along these lines [13] was primarily concerned with the discovery and study of superconducting high-pressure phases in 'natural' superconductors — tallium, lead, and niobium diselenide — as well as in a number of substances that do not exhibit superconducting properties at normal pressure: bismuth, stibium, bismuth–stibium alloys, barium, and some semiconductors and semiconductor compounds (tellurium, bismuth telluride, silicon and germanium, and gallium and indium antimonides). Throughout this list, the superconducting transition temperature of a high pressure phase depends on the type and initial concentration of carriers. As studies under pressure [14] showed, magnetoresistance is a very sensitive means for detecting phase transitions even if electrical resistivity has a small or no jump. This in turn enables using galvanomagnetic measurements to determine the behavior of carrier concentration in each high pressure phase.

The study of the properties of high pressure metastable phases at normal pressure can also be considered part of this area of research. Using high-pressure synthesis, those portions of the phase diagram unachievable at normal pressures can be realized. Sometimes, it is only in this way that some compounds can be produced. In particular, due to the high partial pressure of oxygen or another metalloid it proves possible to get cations that are stabilized in a highly oxidized state. If there is a marked structural rearrangement (for

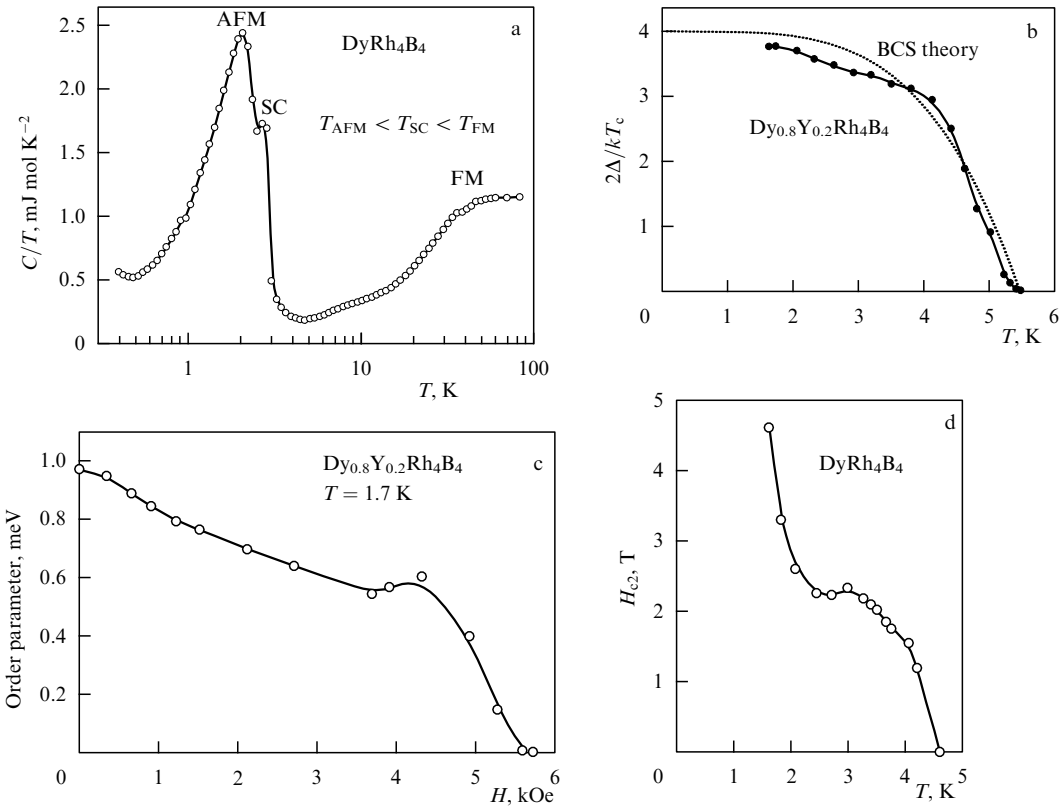

Figure 6. (a) Heat capacity versus temperature for $DyRh_4B_4$. FM, AFM, and SC denote the ferromagnetic, antiferromagnetic, and superconducting transition points, respectively. (b) Measured versus BCS temperature dependence of the energy gap. (c) Field dependence of the order parameter in $Dy_{0.8}Y_{0.2}Rh_4B_4$. (d) Temperature dependence of the second critical field for $DyRh_4B_4$.

example, bond forming or bond breaking) involved in a transition between high- and low-pressure phases, then a 'quenched' metastable state can be obtained by cooling the high pressure stable compound before removing pressure. Such substances include, in particular, perovskite compounds with highly coordinated cations, oxygen-bond-rich compounds, and compounds whose high-pressure phase has a higher symmetry. Examples are the superconductor Nb_3Ge, the T_c-record holder of the 1970s, and mercury-based superconductors, the highest-T_c materials of today. Another important gain from using high pressure in composite material synthesis is the possibility to markedly increase the critical current density, a key characteristic of a superconducting material.

One of the most interesting and important problems in condensed matter physics is to understand how superconductivity and magnetism, two collective macroscopic quantum phenomena, can coexist. Heat capacity versus temperature plots for IHPP-produced metastable high-pressure phases of magnetic superconductors $(Dy,Y)Rh_4B_4$ reveal the existence of three phase transitions: antiferromagnetic, superconducting, and ferromagnetic, with $T_{AFM} < T_{SC} < T_{FM}$ [15].

The temperature dependence of the energy gap differs in both shape and size from what is predicted by the BCS theory. In another finding, the field dependence of the energy gap and the behavior of the second critical field are also far from typical in that in a certain range of magnetic fields the number of superconducting carriers increases, rather than decreases, with field. All this suggests a different superconducting mechanism, possibly one involving triplet pairing (Fig. 6).

This talk covers only part of what high pressure measurements have contributed to the synthesis of appropriate materials and to the understanding of electron transport in systems that involve interactions between the quasiparticles which exist in the electron, phonon, and spin subsystems and whose properties, in turn, can be strongly dependent of the presence of crystal lattice defects. The arsenal of measurement tools includes resistive, tunneling, galvanomagnetic, thermoelectric, electron-optic, and neutron diffraction measurements under pressure. This research is the main focus of activities of the Laboratory of Low Temperatures, which is genetically related to the IHPP divisions mentioned above and which works along these lines in close cooperation with the Institute of Radioengineering and Electronics, RAS, and the Laboratory of Strong Magnetic Fields, Polish Academy of Sciences, under support from RFBR and the RAS Presidium Program.

References

1. Arkhipov R G et al. *Zh. Eksp. Teor. Fiz.* **44** 1964 (1963) [*Sov. Phys. JETP* **17** 1321 (1963)]
2. Itskevich E S, Voronovskii A N *Pis'ma Zh. Eksp. Teor. Fiz.* **4** 226 (1966) [*JETP Lett.* **4** 154 (1966)]
3. Itskevich E S, Gapotchenko A G, Voronovskii A N, Bud'ko S L *Zh. Eksp. Teor. Fiz.* **86** 778 (1984) [*Sov. Phys. JETP* **59** 454 (1984)]
4. Venttsel' V A et al. *Zh. Eksp. Teor. Fiz.* **65** 2445 (1973) [*Sov. Phys. JETP* **38** 1220 (1974)]; Budarin A G, Venttsel' V A, Rudnev A V *Zh. Eksp. Teor. Fiz.* **75** 1706 (1978) [*Sov. Phys. JETP* **48** 858 (1978)]
5. Budarin A G, Venttsel' V A, Rudnev A V *Fiz. Nizk. Temp.* **12** 312 (1986) [*Sov. J. Low Temp. Phys.* **12** 177 (1986)]

6. Venttsel' V A, Kochkin A P, Rudnev A V *Fiz. Nizk. Temp.* **13** 484 (1987) [*Sov. J. Low Temp. Phys.* **13** 273 (1987)]
7. Kraidenov V F, Itskevich E S *Fiz. Tverd. Tela* **37** 405 (1995)
8. Zavaritskii N V, Itskevich E S, Voronovskii A N *Zh. Eksp. Teor. Fiz.* **60** 1408 (1971) [*Sov. Phys. JETP* **33** 762 (1971)]
9. Voronovskii A N, Dizhur E M , Itskevich E S *Zh. Eksp. Teor. Fiz.* **77** 1119 (1979) [*Sov. Phys. JETP* **50** 564 (1979)]
10. Voronovskii A N et al. *Fiz. Tverd. Tela* **39** 723 (1997) [*Phys. Solid State* **39** 637 (1997)]
11. Dizhur E M et al. *Pis'ma Zh. Eksp. Teor. Fiz.* **80** 489 (2004) [*JETP Lett.* **80** 433 (2004)]
12. Dizhur E M, Il'ina M A, Zaitsev-Zotov S V *Pis'ma Zh. Eksp. Teor. Fiz.* **86** 141 (2007) [*JETP Lett.* **86** 132 (2007)]
13. Il'ina M A, Itskevich E S *Fiz. Tverd. Tela* **17** 154 (1975)
14. Venttsel V A et al. *Fiz. Tverd. Tela* **20** 3178 (1978)
15. Burkhanov G S et al. *Neorg. Mater.* **41** 676 (2005) [*Inorganic Mater.* **41** 585 (2005)]

PACS numbers: **71.15.–m**, **74.20.–z**, **75.10.–b**
DOI: 10.1070/PU2008v051n10ABEH006619

Theoretical studies of condensed matter

V N Ryzhov, A F Barabanov, M V Magnitskaya, E E Tareyeva

This talk briefly reviews the basic directions the Theoretical Department of the Institute for High Pressure Physics, RAS, (IHPP) has been pursuing in condensed matter research during the 50-year existence of the institute.

In the 1960s, the IHPP Theoretical Department became one of the first research centers in our country to employ first principle computational methods — i.e., ones that involve no fitting parameters and thus are experiment-independent — to study the physical properties of and phase transformations in solids, in particular under high pressure conditions. This research is usually carried out in close cooperation with experimenters using experiment/theory comparisons to clarify the underlying physics of the phenomena being observed. Along with known materials, new high-pressure phases first obtained at the IHPP are being investigated. Starting in the 1960s and 1970s, appropriate computational techniques using electron density functional theory, such as the Augmented Plane Wave and Korringa–Kohn–Rostoker methods and their modifications and extensions, have been further developed and revised by IHPP theorists.

The early work by R G Arkhipov, E S Alekseev, and A P Kochkin [1] used the approximate Wigner–Seitz spherical cell method, with a unit cell replaced by an equal-sized sphere, to study the relation between the electronic structure and phase transformations in simple metals under high pressure at $T = 0$. A major finding of this study, a phase transition with a volume change in K, Rb, and Cs, was explained in terms of an electron s–d transition, i.e., as resulting from a pressure-induced change in the mutual arrangement the of s and d bands. The discovery, made due to advances in experimental techniques, and subsequent studies of new low-symmetry high-pressure phases in simple metals brought fresh relevance to this line of research. At present, IHPP researchers use modern theoretical methods (in particular, based on the first-principle pseudopotentials) not only to exactly determine structural sequences in simple metals under pressure at $T = 0$, but also to study $P - T$ phase diagrams at finite temperatures $T \neq 0$, on the basis of the phonon spectra calculations by the density-functional linear-response method [2].

The IHPP's M V Magnitskaya and colleagues from outside Russia [3] have calculated the electron and phonon spectra and the electron-phonon coupling (EPC) for a recently discovered high-pressure metallic phase of sulphur S-IV, which exhibits the incommensurate modulation of atomic positions in the direction [010] (charge density wave, CDW). The first-principle calculation produced a correct crystal structure for the modulated phase of S-IV. The transition to the CDW state can be interpreted as a distortion of the higher-density S-V phase (which has the β-Po type crystal structure). The results of calculations show that in the β-Po structure one of the transverse phonon modes on the vector $\mathbf{q}_{\mathrm{CDW}}$ becomes softer with decreasing pressure. Upon further decrease in pressure to $P \approx 135$ GPa, the frequency of this mode becomes zero, $\omega(\mathbf{q}_{\mathrm{CDW}}) = 0$, corresponding to the S-V phase being unstable relative to the transition to the S-IV phase in which this unstable phonon is 'frozen' into a CDW. The location of the minimum of the phonon mode is in excellent agreement with the experimental modulation vector $\mathbf{q}_{\mathrm{CDW}}$. To analyze the role of the electron–soft mode coupling, the contributions from various phonon modes to the matrix elements of the EPC were calculated. It has been established that the soft-mode contribution is maximum on the vector $\mathbf{q}_{\mathrm{CDW}}$, suggesting that the experimental jump at $p \approx 150$ GPa from 14 to 17 K in the superconducting transition temperature T_c can be due to the fact that at $p > p_{\mathrm{CDW}}$ the electron density of states at the Fermi level increases and the electron–soft mode coupling contributes significantly to T_c. This jump, as well as the subsequent increase in T_c in the interval to $P \approx 200$ GPa, is explained by the competition between the soft mode frequency $\omega(\mathbf{q}_{\mathrm{CDW}})$ and the electron–phonon coupling constant [3].

In the 1970s, due to improvements in computational techniques, institute theorists started broad-scope studies of transition and rare-earth metals, intermetallic compounds, and alloys, covering in detail pressure-induced magnetic phase transitions, as well as alloying and phase stability, galvanomagnetic effects, optical and photoemission spectra, etc. Of particular note are the studies of the magnetic properties in double and triple Laves phase materials, including new compounds, first synthesized at the IHPP [4], of the magnetic 3d metals Fe, Co, and Ni with calcium. Considerable interest was generated by studies by N I Kulikov and colleagues of the effect of pressure on the properties of magnetically ordered metals and alloys, including complex — incommensurate and noncollinear — antiferromagnetic (AFM) structures, for example, chromium and yttrium and their respective alloys, the systems Pt_3Fe, FeRh, etc. [5]. In this context, the excitonic dielectric model combined with band calculations proved a very fruitful approach, offering a single framework for explaining how congruent Fermi surface regions give rise to various AFM orderings. For chromium, in which AFM ordering can be thought of as an incommensurate spin density wave the AFM-destroying effect of the EPC was investigated [6]. A series of publications by N I Kulikov and coworkers on the development of the coherent potential method and its application to disordered systems examined in detail the relation between structural disordering and the magnetic properties for various binary alloys of transition metals and for the disordered alloys of 3d metals with Si, Al, etc. [7].

Finally, one more area of research that emerged in the 1970s was the study of the compounds — carbides, nitrides, hydrides, etc. — which transition and rare earth metals form